

# Lipid Expansion Microscopy

Brittany M. White<sup>1,2</sup>, Amanda N. Conwell<sup>1,2\*</sup>, Kane Wu<sup>1,2\*</sup>, and Jeremy M. Baskin<sup>1,2†</sup>

<sup>1</sup>Department of Chemistry and Chemical Biology, Cornell University, Ithaca NY 14853 USA

<sup>2</sup>Weill Institute for Cell and Molecular Biology, Cornell University, Ithaca NY 14853 USA

\* These authors contributed equally

† Correspondence: jeremy.baskin@cornell.edu

## ABSTRACT

Strategies to visualize cellular membranes with light microscopy are restricted by the diffraction limit of light, which far exceeds the dimensions of lipid bilayers. Here, we describe a method for super-resolution imaging of metabolically labeled phospholipids within cellular membranes. Guided by the principles of expansion microscopy, we develop an approach featuring cell-permeable reagents that enables direct chemical anchoring of bioorthogonally labeled phospholipids into a hydrogel network and is capable of tunable, isotropic expansion, thus facilitating super-resolution imaging of cellular membranes. We apply this method, termed lipid expansion microscopy, to visualize organelle membranes with precision, including a unique class of membrane-bound structures known as nuclear invaginations. As it is compatible with standard confocal microscopes, lipid expansion microscopy will be widely applicable for super-resolution imaging of phospholipids and cellular membranes in numerous physiological contexts.

## MAIN TEXT

Biological membranes have many essential functions, most fundamentally to encapsulate cells and organelles. The formation of membranous structures such as invaginations and protrusions, inter-organelle contact sites, and microdomains are critical for cell trafficking and signaling events.<sup>1,2</sup> Membranes are primarily composed of phospholipids, making methods to visualize these biomolecules vital to understanding cellular functions.<sup>3-5</sup> However, techniques to accurately image phospholipids with fluorescence microscopy are challenged the by the impermeable nature of the membrane and dimensions of the lipid bilayer, which are smaller than the diffraction limit of light.<sup>6</sup>

Super-resolution imaging techniques including stimulated emission depletion (STED) and single-molecule localization microscopy (SMLM) can surpass the diffraction limit and enable imaging of lipids within membranes.<sup>7-10</sup> However, these techniques require specialized setups and procedures, limiting such imaging to laboratories with the required instrumentation and expertise. Expansion microscopy (ExM) has emerged as a powerful and accessible alternative super-resolution imaging strategy, wherein target biomolecules are anchored to a hydrogel network that is swollen to expand the physical size of a sample by  $\sim 5x$ , spatially separating signal and enabling high-resolution imaging with standard fluorescence microscopes.<sup>11-15</sup> Specialized versions of ExM can increase the expansion factor to 15x, enabling imaging of a wide variety of cellular structures in situ.<sup>16-22</sup> Though traditional ExM protocols involve permeabilization, and thus lipid removal, prior to expansion and imaging, certain adaptations have allowed for imaging of membranes. For example, unnatural crosslinkable hydrophobic probes can intercalate into membranes, mimicking natural lipids and allowing retention for ExM imaging.<sup>23-26</sup> Alternatively, metabolic labeling of native phospholipids has also been leveraged for expansion of membranes using click-ExM, which anchors lipids to the hydrogel network through a biotin-streptavidin conjugation.<sup>27</sup> Notably, these methods require at least mild permeabilization of the membrane, which can compromise its integrity and potentially alter its structure, to ensure a uniform distribution of ExM reagents and isotropic expansion of samples.

We were motivated by a desire to visualize lipids using ExM with molecular detail while preserving the structural integrity of the membranes. Here, we present an approach involving metabolic labeling of natural phospholipids, a trifunctional fluorophore for the tagging and tethering of lipids to the hydrogel, and membrane-permeable expansion reagents (Figure 1A). This method, termed Lipid Expansion Microscopy (LExM), allows for the tunable and isotropic expansion of membranes through direct anchoring of phospholipids into the polymer network without permeabilization. We demonstrate that LExM is a general method for the expansion of metabolically labeled lipids to enable super-resolution imaging of organelle membranes, and we apply LExM to visualize sub-diffraction scale invaginations of the nuclear membrane and their membrane-bound cytoplasmic contents.

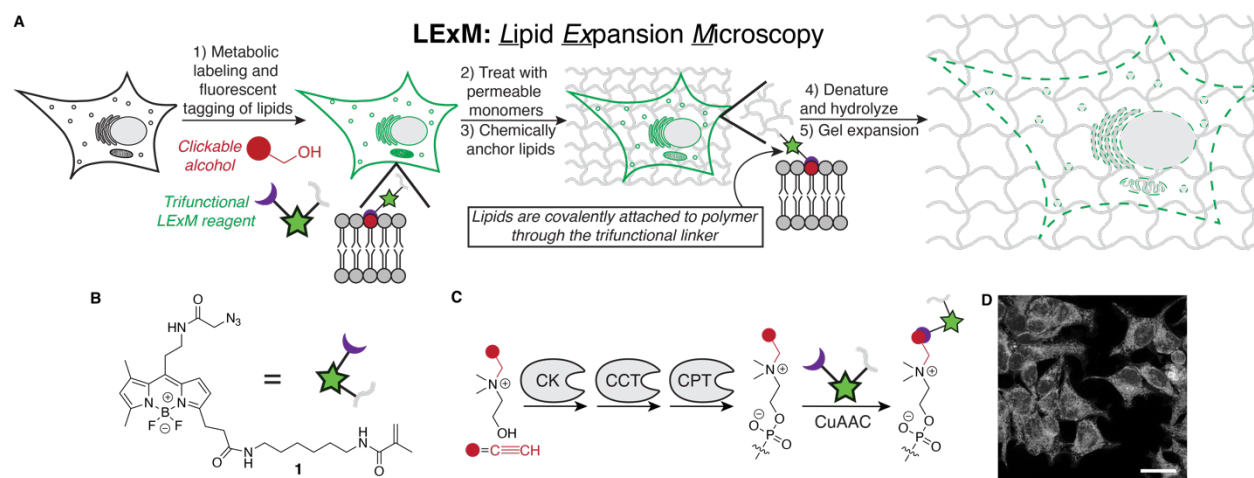


**Figure 1.** (A) Scheme of lipid expansion microscopy (LExM). (B) Structure of trifunctional reagent **1**. (C) Propargylcholine (ProCho) incorporation into phospholipids through the Kennedy pathway. CK: choline kinase, CCT: CTP:phosphocholine cytidyltransferase, CPT: cholinephosphotransferase. (D) Confocal imaging of cells metabolically labeled with ProCho and tagged with **1** via CuAAC. Scale bar: 30  $\mu\text{m}$ .

To incorporate phospholipids directly into the hydrogel network, we designed and prepared trifunctional LExM reagent **1** (Figure 1B), which is equipped with (i) an azido group for tagging alkyne-labeled biomolecules via Cu-catalyzed azide-alkyne cycloaddition (CuAAC), (ii) a BODIPY fluorophore for imaging pre- and post-LExM, and (iii) a methacrylamide polymerizable unit for direct incorporation into the hydrogel network. We validated that **1** is membrane-permeable and capable of imaging bioorthogonally labeled lipids by confocal microscopy imaging of HeLa cells tagged with **1** after treatment with propargylcholine (ProCho), an alkynyl analog of choline that is metabolically incorporated into phosphatidylcholine (PC) and other choline-containing lipids (Figure 1C).<sup>28</sup> We observed a strong fluorescent signal from many intracellular membranes, consistent with the broad distribution of PC in mammalian cells (Figure 1D). Importantly, the signal was ProCho-dependent, indicating that **1** is specific for alkyne-labeled phospholipids (Figure S1).

A key feature of ExM is isotropic sample expansion, which is achieved by disrupting membranes with permeabilization to enable uniform diffusion of polymerization reagents throughout the sample.<sup>29</sup> This step is critical for incorporation of ionic monomers needed for the final osmotic expansion step, and for streptavidin-based anchoring strategies where such macromolecular fluorescent labeling reagents are membrane-impermeable.<sup>15,26,27</sup> To ensure that

monomers are evenly distributed in LExM, we used uncharged, membrane-permeable monomers that are hydrolyzed, post-polymerization, to yield ionic residues necessary for expansion.<sup>21</sup>

Our optimized LExM protocol involves metabolic labeling of cells with ProCho, fixation, fluorescent tagging with **1** via CuAAC, polymerization in the presence of acrylamide and bis-acrylamide monomers, denaturation and hydrolysis, and finally expansion, followed by visualization by traditional or Airyscan confocal microscopy (Figure 1A). Excitingly, we observed signal from expanded samples, demonstrating that **1** is a suitable chemical anchor that directly incorporates labeled lipids into the hydrogel network (Figure 2A). Using a 4 h hydrolysis step, LExM afforded a 6.8x expansion factor, enabling visualization of fine structures, e.g., the nuclear envelope, which is clearly distinguished from other intracellular membranes (Figures 2B–C).

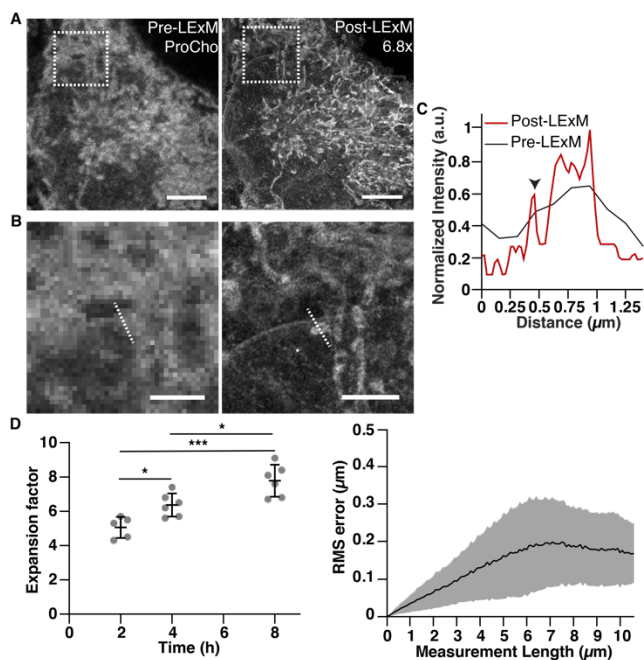


**Figure 2.** (A) Confocal images of the same cell metabolically labeled with ProCho pre-LExM (left) and post-LExM (right). Expansion factor is displayed in the upper right corner of the post-LExM image. (B) Pre-LExM (left) and post-LExM (right) boxed areas in A. Scale bars (pre-LExM distance): 5  $\mu\text{m}$  (A), 2  $\mu\text{m}$  (B). (C) Fluorescence intensity profile line plots for dotted lines in pre- and post-LExM images. Arrowhead indicates nuclear envelope. (D) Expansion factors of samples hydrolyzed for 2, 4 and 8 h (left). Statistical significance: ANOVA (one-way, Tukey). \*  $p < 0.05$ , \*\*\*  $p < 0.001$ . Root mean square (RMS) error as a function of measurement length generated by non-rigid registration of pre- and post-LExM images (right,  $n=6$ ).

Next, we assessed the ability of LExM to expand samples in a tunable and isotropic fashion. We varied the acrylamide to acrylate hydrolysis time and compared pre- and post-LExM images

of the same area using rigid registration to determine expansion factors. Hydrolysis times of 2, 4, and 8 h gave expansion factors of  $\sim 5.0x$ ,  $\sim 6.4x$  and  $\sim 7.8x$  respectively, confirming that LExM enables the tunable expansion of membranes (Figure 2D). Comparison of pre- and post-LExM images with non-rigid registration revealed minimal distortion of samples, with a root mean square (RMS) error of  $<3\%$  for distances of up to  $10\ \mu\text{m}$ , demonstrating that LExM enables the isotropic expansion of tagged lipids (Figure 2D).

We next sought to harness the enhanced resolution afforded by LExM to identify the locations of metabolically labeled PC, an analysis that is challenged by the broad distribution of this phospholipid and the close juxtaposition of organelles at membrane contact sites.<sup>30</sup> This goal required adaptation of LExM to enable colocalization studies with organelle markers using immunofluorescence. Comparisons of pre- and post-LExM images of cells immunostained for a transfected ER marker revealed that areas with high colocalization could be clearly delineated from other closely associated membranes in the post-LExM image at a level of detail absent in the pre-LExM image (Figure 3A). An examination of representative line plots of fluorescent profiles from each image showed clear peaks separated by  $\sim 100\ \text{nm}$  in the post-LExM image, in contrast to peaks  $\sim 300\ \text{nm}$  width in the pre-LExM image. Similar increases in resolution were seen in post-LExM images of labeled PC with markers of the Golgi complex and mitochondria (Figures 3B–C), with the latter enabling specific visualization of the outer mitochondrial membrane compared to other associated membranes containing tagged PC.<sup>31</sup> Together, these colocalization experiments demonstrate the ability of LExM to generate super-resolution images that can precisely identify the locations of PC-containing membranes.

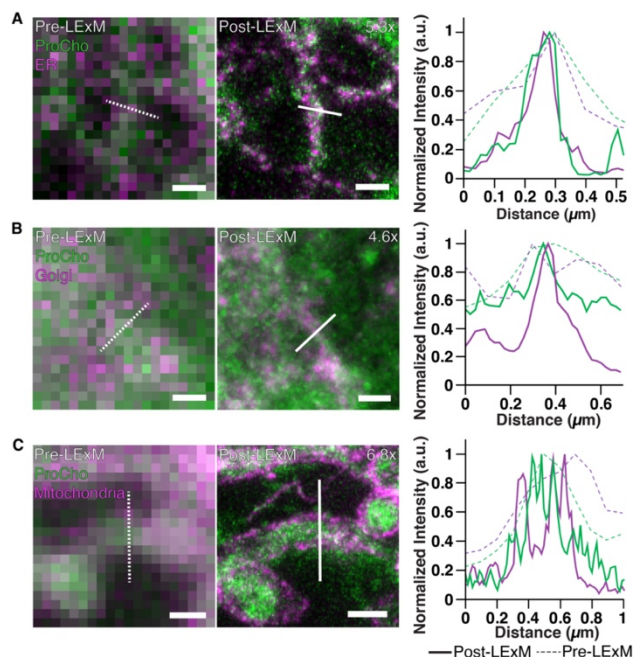


**Figure 3.** Pre- (left) and post-LExM (middle) Airyscan confocal images of a cell transfected with organelle marker (magenta; mRFP-Sec61 $\beta$ , ER (A); mCherry-PH(OSBP), Golgi complex (B); OMP25TM-mCherry, mitochondria (C)) then metabolically labeled with ProCho (green), with fluorescence intensity profile line plots of the pre- (dotted line) and post-LExM (solid line) images. Expansion factors are displayed in the upper right corner of post-LExM images. Dotted and solid lines on images indicate profiles measured for line plots. Scale bars (pre-LExM distance): 400 nm.

Whereas metabolic labeling of phospholipids with ProCho enables measurement of bulk membrane lipids, many important signaling phospholipids, such as phosphatidic acid (PA), are generated at much lower levels.<sup>32</sup> We have developed a method termed IMPACT to visualize the activity of phospholipase Ds (PLDs), which generate PA, by leveraging the ability of these enzymes to attach bioorthogonally labeled primary alcohols onto phospholipids in a transphosphatidylation, or head group exchange, reaction (Figure 4A).<sup>33–36</sup> To establish LExM as a more general strategy for ExM-based imaging of alkyne-labeled lipids, we subjected cells to IMPACT labeling with the PLD substrate hexynol, CuAAC tagging with **1**, and the LExM protocol. Consistent with the ProCho-based LExM studies, IMPACT labeling generated samples with a 5.6x expansion factor (at the 4 h hydrolysis timepoint) and fluorescence signal that correlated well with the pre-LExM image (Figure 4B). The enhanced resolution of the post-LExM image also enabled identification of distinct membranes in crowded areas, e.g., the nuclear envelope (Figure 4B–C). Samples generated with IMPACT were similarly obtained in a tunable manner with isotropic expansion and were amenable to colocalization studies with organelle

markers (Figures S2–S3). Importantly, treatment with a pan-PLD inhibitor prevented fluorescent labeling in pre-LExM images (Figure S2).

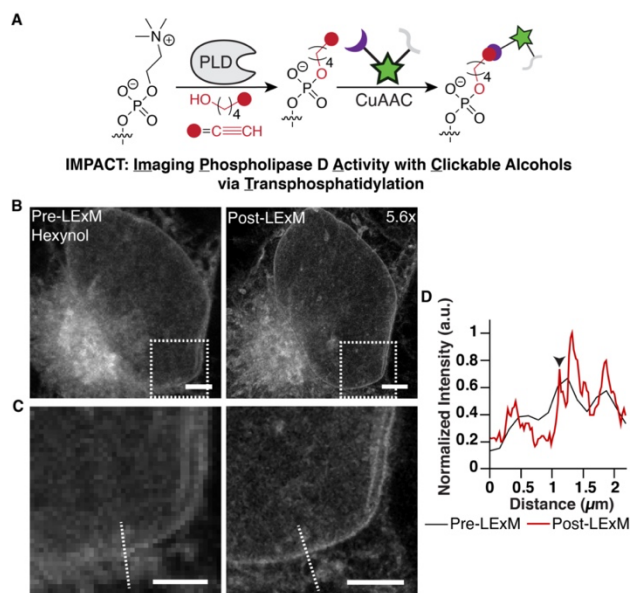


**Figure 4.** (A) Cells were labeled via IMPACT in the presence of hexynol followed by CuAAC tagging with **1**. (B) Pre- (left) and post-LExM (right) confocal images of cells labeled with hexynol. Expansion factor is displayed in the upper right corner of the post-LExM image. (C) Pre-LExM (left) and post-LExM (right) boxed areas in A. Scale bars (pre-LExM distance): 3  $\mu\text{m}$  (A), 2  $\mu\text{m}$  (B). (D) Fluorescence intensity profile line plot for dotted lines in pre- (black) and post-LExM (red) images. Arrowhead indicates nuclear envelope.

Finally, we applied LExM to study specific sub-diffraction scale cellular structures. Metabolic labeling of phospholipids revealed channels that traverse nuclei, which we hypothesized were a unique class of structures known as nuclear invaginations (Video S1). These channels, comprised of nuclear membrane surrounded by lamina that envelop cytoplasmic contents, can travel through nuclei.<sup>37,38</sup> Because of their narrow dimensions, their detailed analysis has been limited to electron microscopy and traditional super-resolution microscopy (e.g., STED/SMLM).<sup>7,8,39,40</sup> To visualize these membrane-bound structures with ExM, we labeled cells expressing a nuclear lamina marker with ProCho and performed the LExM protocol. Inspection of post-ExM images revealed channels that were surrounded by lamina, confirming their identity as nuclear invaginations (Figure 5A). Analysis of fluorescent profiles across individual channels revealed fluorescence signal from metabolically labeled lipids in the center of the channel, suggesting that LExM can identify intact cytoplasmic organelles contained within these nuclear

invaginations (Figure 5A). Indeed, cells labeled by LExM exhibited strong colocalization of an ER marker and ProCho within the channel (Figure 5B). Further, we detected similar large nuclear invaginations in IMPACT-labeled samples co-labeled with a mitochondrial marker, in which the outer mitochondrial membrane could be distinguished from other associated membranes within the channel (Figure 5C). Collectively, these experiments indicate that LExM, with multiple types of metabolic and organelle labels, can detect organelles associated with nuclear invaginations, demonstrating LExM as a powerful method for detailed analysis of intracellular structures.

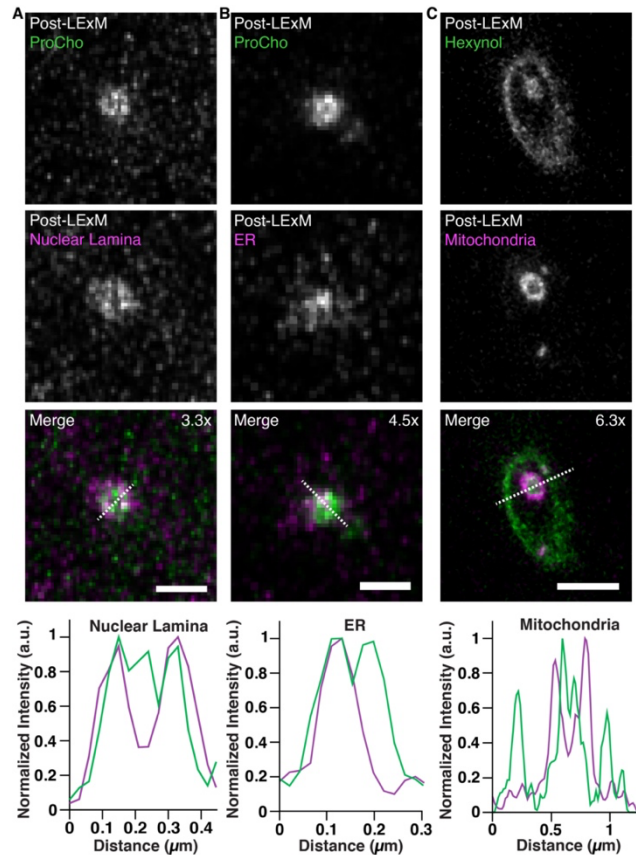


**Figure 5.** Cells were transfected with organelle markers (mRFP-Lamin A, nuclear lamina (A); mRFP-Sec61 $\beta$ , ER (B); OMP25TM-mCherry, mitochondria (C)) and metabolically labeled with ProCho (A–B) or hexynol via IMPACT (C). Fluorescent intensity profile line plots generated from dotted line in merge images. Airyscan confocal images are zoom-ins focused on nuclear channels with metabolic labeling of lipids (left, green in merge), organelle markers (middle, magenta in merge), and merged image (right, colocalization appears as white). Expansion factors are displayed in the upper right corner of merged images. Scale bars (pre-LExM distance): 500 nm (A), 300 nm (B), and 1  $\mu$ m (C).

In summary, LExM is a general method for super-resolution imaging of lipid species within cellular membranes. It exploits cell-permeable reagents that enable direct anchoring of metabolically labeled lipids to a hydrogel network, permitting tunable and isotropic expansion without detergent-based permeabilization, to preserve and illuminate molecular and structural details. LExM is compatible with metabolic labels both for bulk phospholipids and low-abundant signaling lipids, enabling high-resolution visualization of organelle membranes and subcellular structures with dimensions smaller than the diffraction limit of light. With accessible reagents and requiring only a standard confocal microscope, we envision that LExM will democratize high-resolution imaging of lipids and membranes. Further, the reagents developed for LExM should be useful for ExM-based high-resolution imaging of metabolites, small-molecule biosensors, glycans, and other protein posttranslational modifications amenable to bioorthogonal metabolic or chemoenzymatic labeling.

## **ACKNOWLEDGMENTS**

J.M.B. acknowledges support from the Arnold and Mabel Beckman Foundation (Beckman Young Investigator Award) and the Alfred P. Sloan Foundation (Sloan Research Fellowship). B.M.W. acknowledges support from the National Institutes of Health (F32GM134632). This work made use of the Cornell University NMR Facility, which is supported in part by the NSF (CHE-1531632). We thank Jan Lammerding for supplies and Timothy Bumpus, Marshall Colville, and Matthew Paszek for helpful discussions.

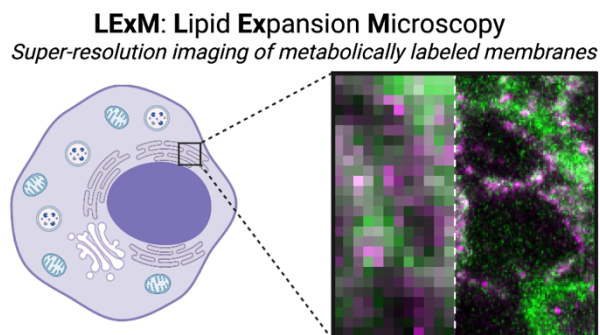
## **AUTHOR CONTRIBUTIONS**

B.M.W. and J.M.B. designed experiments, analyzed results, and wrote the manuscript. B.M.W. performed all experiments, image processing, and data analysis. A.N.C. and K.W. performed organic synthesis.

## **CONFLICTS OF INTEREST**

The authors declare no conflicts of interest.

## TOC GRAPHIC



## REFERENCES

- (1) Harayama, T.; Riezman, H. Understanding the Diversity of Membrane Lipid Composition. *Nat. Rev. Mol. Cell Biol.* **2018**, *19* (5), 281–296.
- (2) Prinz, W. A.; Toulmay, A.; Balla, T. The Functional Universe of Membrane Contact Sites. *Nat. Rev. Mol. Cell Biol.* **2019**, *21* (1), 7–24.
- (3) Vance, J. E. Phospholipid Synthesis and Transport in Mammalian Cells. *Traffic* **2015**, *16* (1), 1–18.
- (4) Bumpus, T. W.; Baskin, J. M. Greasing the Wheels of Lipid Biology with Chemical Tools. *Trends Biochem. Sci.* **2018**, *43* (12), 970–983.
- (5) Flores, J.; White, B. M.; Brea, R. J.; Baskin, J. M.; Devaraj, N. K. Lipids: Chemical Tools for Their Synthesis, Modification, and Analysis. *Chem. Soc. Rev.* **2020**, *49* (14), 4602–4614.
- (6) Yang, N. J.; Hinner, M. J. Getting Across the Cell Membrane: An Overview for Small Molecules, Peptides, and Proteins. *Methods Mol. Biol.* **2015**, *1266*, 29–53.
- (7) Thompson, A. D.; Bewersdorf, J.; Toomre, D.; Schepartz, A. HIDE Probes: A New Toolkit for Visualizing Organelle Dynamics, Longer and at Super-Resolution. *Biochemistry* **2017**, *56* (39), 5194–5201.
- (8) Takakura, H.; Zhang, Y.; Erdmann, R. S.; Thompson, A. D.; Lin, Y.; McNellis, B.; Rivera-Molina, F.; Uno, S. N.; Kamiya, M.; Urano, Y.; Rothman, J. E.; Bewersdorf, J.; Schepartz, A.; Toomre, D. Long Time-Lapse Nanoscopy with Spontaneously Blinking Membrane Probes. *Nat. Biotechnol.* **2017**, *35* (8), 773–780.
- (9) Gupta, A.; Rivera-Molina, F.; Xi, Z.; Toomre, D.; Schepartz, A. Endosome Motility Defects Revealed at Super-Resolution in Live Cells Using HIDE Probes. *Nat. Chem. Biol.* **2020**, *16* (4), 408–414.
- (10) Dadina, N.; Tyson, J.; Zheng, S.; Lesiak, L.; Schepartz, A. Imaging Organelle Membranes in Live Cells at the Nanoscale with Lipid-Based Fluorescent Probes. *Curr. Opin. Chem. Biol.* **2021**, *65*, 154–162.
- (11) Chen, F.; Tillberg, P. W.; Boyden, E. S. Expansion Microscopy. *Science* **2015**, *347* (6221), 543–548.
- (12) Chozinski, T. J.; Halpern, A. R.; Okawa, H.; Kim, H. J.; Tremel, G. J.; Wong, R. O. L.; Vaughan, J. C. Expansion Microscopy with Conventional Antibodies and Fluorescent Proteins. *Nat. Methods* **2016**, *13* (6), 485–488.
- (13) Ku, T.; Swaney, J.; Park, J. Y.; Albanese, A.; Murray, E.; Hun Cho, J.; Park, Y. G.;

- Mangena, V.; Chen, J.; Chung, K. Multiplexed and Scalable Super-Resolution Imaging of Three-Dimensional Protein Localization in Size-Adjustable Tissues. *Nat. Biotechnol.* **2016**, *34* (9), 973–981.
- (14) Wassie, A. T.; Zhao, Y.; Boyden, E. S. Expansion Microscopy: Principles and Uses in Biological Research. *Nat. Methods* **2018**, *16* (1), 33–41.
- (15) Asano, S. M.; Gao, R.; Wassie, A. T.; Tillberg, P. W.; Chen, F.; Boyden, E. S. Expansion Microscopy: Protocols for Imaging Proteins and RNA in Cells and Tissues. *Curr. Protoc. Cell Biol.* **2018**, *80* (1), e56.
- (16) Truckenbrodt, S.; Maidorn, M.; Crzan, D.; Wildhagen, H.; Kabatas, S.; Rizzoli, S. O. X10 Expansion Microscopy Enables 25-Nm Resolution on Conventional Microscopes. *EMBO Rep.* **2018**, *19* (9), e45836.
- (17) Chang, J. B.; Chen, F.; Yoon, Y. G.; Jung, E. E.; Babcock, H.; Kang, J. S.; Asano, S.; Suk, H. J.; Pak, N.; Tillberg, P. W.; Wassie, A. T.; Cai, D.; Boyden, E. S. Iterative Expansion Microscopy. *Nat. Methods* **2017**, *14* (6), 593–599.
- (18) Truckenbrodt, S.; Sommer, C.; Rizzoli, S. O.; Danzl, J. G. A Practical Guide to Optimization in X10 Expansion Microscopy. *Nat. Protoc.* **2019**, *14* (3), 832–863.
- (19) Wen, G.; Vanheusden, M.; Leen, V.; Rohand, T.; Vandereyken, K.; Voet, T.; Hofkens, J. A Universal Labeling Strategy for Nucleic Acids in Expansion Microscopy. *J. Am. Chem. Soc.* **2021**, *143* (34), 13782–13789.
- (20) Chen, F.; Wassie, A. T.; Cote, A. J.; Sinha, A.; Alon, S.; Asano, S.; Daugharthy, E. R.; Chang, J. B.; Marblestone, A.; Church, G. M.; Raj, A.; Boyden, E. S. Nanoscale Imaging of RNA with Expansion Microscopy. *Nat. Methods* **2016**, *13* (8), 679–684.
- (21) Park, H.; Choi, D.; Park, J. S.; Sim, C.; Park, S.; Kang, S.; Yim, H.; Lee, M.; Kim, J.; Pac, J.; Rhee, K.; Lee, J.; Lee, Y.; Lee, Y.; Kim, S.-Y. Scalable and Isotropic Expansion of Tissues with Simply Tunable Expansion Ratio. *Adv. Sci.* **2019**, *6* (22), 1901673.
- (22) Shi, X.; Li, Q.; Dai, Z.; Tran, A. A.; Feng, S.; Ramirez, A. D.; Lin, Z.; Wang, X.; Chow, T. T.; Chen, J.; Kumar, D.; McColloch, A. R.; Reiter, J. F.; Huang, E. J.; Seiple, I. B.; Huang, B. Label-Retention Expansion Microscopy. *J. Cell Biol.* **2021**, *220* (9).
- (23) Karagiannis, E. D.; Kang, J. S.; Shin, T. W.; Emenari, A.; Asano, S.; Lin, L.; Costa, E. K.; Consortium, I. G. C.; Marblestone, A. H.; Kasthuri, N.; Boyden, E. S. Expansion Microscopy of Lipid Membranes. *bioRxiv* **2019**, 829903. <https://doi.org/10.1101/829903>.
- (24) Götz, R.; Kunz, T. C.; Fink, J.; Solger, F.; Schlegel, J.; Seibel, J.; Kozjak-Pavlovic, V.; Rudel, T.; Sauer, M. Nanoscale Imaging of Bacterial Infections by Sphingolipid Expansion Microscopy. *Nat. Commun.* **2020**, *11*, 6173.
- (25) Wen, G.; Vanheusden, M.; Acke, A.; Valli, D.; Neely, R. K.; Leen, V.; Hofkens, J. Evaluation of Direct Grafting Strategies via Trivalent Anchoring for Enabling Lipid Membrane and Cytoskeleton Staining in Expansion Microscopy. *ACS Nano* **2020**, *14* (7), 7377–7387.
- (26) Damstra, H. G. J.; Mohar, B.; Eddison, M.; Akhmanova, A.; Kapitein, L. C.; Tillberg, P. W. Visualizing Cellular and Tissue Ultrastructure Using Ten-Fold Robust Expansion Microscopy (TReX). *Elife* **2022**, *11*, e73775.
- (27) Sun, D. en; Fan, X.; Shi, Y.; Zhang, H.; Huang, Z.; Cheng, B.; Tang, Q.; Li, W.; Zhu, Y.; Bai, J.; Liu, W.; Li, Y.; Wang, X.; Lei, X.; Chen, X. Click-ExM Enables Expansion Microscopy for All Biomolecules. *Nat. Methods* **2020**, *18* (1), 107–113.
- (28) Jao, C. Y.; Roth, M.; Welti, R.; Salic, A. Metabolic Labeling and Direct Imaging of Choline Phospholipids in Vivo. *Proc. Natl. Acad. Sci. U. S. A.* **2009**, *106* (36), 15332–15337.

- (29) Gao, R.; Yu, C. C. (Jay); Gao, L.; Piatkevich, K. D.; Neve, R. L.; Munro, J. B.; Upadhyayula, S.; Boyden, E. S. A Highly Homogeneous Polymer Composed of Tetrahedron-like Monomers for High-Isotropy Expansion Microscopy. *Nat. Nanotechnol.* **2021**, *16* (6), 698–707.
- (30) Zhanghao, K.; Liu, W.; Li, M.; Wu, Z.; Wang, X.; Chen, X.; Shan, C.; Wang, H.; Chen, X.; Dai, Q.; Xi, P.; Jin, D. High-Dimensional Super-Resolution Imaging Reveals Heterogeneity and Dynamics of Subcellular Lipid Membranes. *Nat. Commun.* **2020**, *11*, 5890.
- (31) Tamura, T.; Fujisawa, A.; Tsuchiya, M.; Shen, Y.; Nagao, K.; Kawano, S.; Tamura, Y.; Endo, T.; Umeda, M.; Hamachi, I. Organelle Membrane-Specific Chemical Labeling and Dynamic Imaging in Living Cells. *Nat. Chem. Biol.* **2020**, *16* (12), 1361–1367.
- (32) Selvy, P. E.; Lavieri, R. R.; Lindsley, C. W.; Brown, H. A. Phospholipase D: Enzymology, Functionality, and Chemical Modulation. *Chem. Rev.* **2011**, *111* (10), 6064–6119.
- (33) Bumpus, T. W.; Baskin, J. M. A Chemoenzymatic Strategy for Imaging Cellular Phosphatidic Acid Synthesis. *Angew. Chemie Int. Ed.* **2016**, *55* (42), 13155–13158.
- (34) Bumpus, T. W.; Baskin, J. M. Clickable Substrate Mimics Enable Imaging of Phospholipase D Activity. *ACS Cent. Sci.* **2017**, *3* (10), 1070–1077.
- (35) Liang, D.; Wu, K.; Tei, R.; Bumpus, T. W.; Ye, J.; Baskin, J. M. A Real-Time Click Chemistry Imaging Approach Reveals Stimulus-Specific Subcellular Locations of Phospholipase D Activity. *Proc. Natl. Acad. Sci. U. S. A.* **2019**, *116* (31), 15453–15462.
- (36) Tei, R.; Baskin, J. M. Click Chemistry and Optogenetic Approaches to Visualize and Manipulate Phosphatidic Acid Signaling. *J. Biol. Chem.* **2022**, 101810. <https://doi.org/10.1016/J.JBC.2022.101810>.
- (37) Drozd, M. M.; Jiang, H.; Pytowski, L.; Grovenor, C.; Vaux, D. J. Formation of a Nucleoplasmic Reticulum Requires de Novo Assembly of Nascent Phospholipids and Shows Preferential Incorporation of Nascent Lamins. *Sci. Rep.* **2017**, *7* (1), 1–14.
- (38) Schoen, I.; Aires, L.; Ries, J.; Vogel, V. Nanoscale Invaginations of the Nuclear Envelope: Shedding New Light on Wormholes with Elusive Function. *Nucleus* **2017**, *8* (5), 506–514.
- (39) Fricker, M.; Hollinshead, M.; White, N.; Vaux, D. Interphase Nuclei of Many Mammalian Cell Types Contain Deep, Dynamic, Tubular Membrane-Bound Invaginations of the Nuclear Envelope. *J. Cell Biol.* **1997**, *136* (3), 531–544.
- (40) Mateusz, M.; David, D. & Vaux, J.; Drozd, M.; Vaux, D. J. Shared Mechanisms in Physiological and Pathological Nucleoplasmic Reticulum Formation. *Nucleus* **2017**, *8* (1), 34–45.